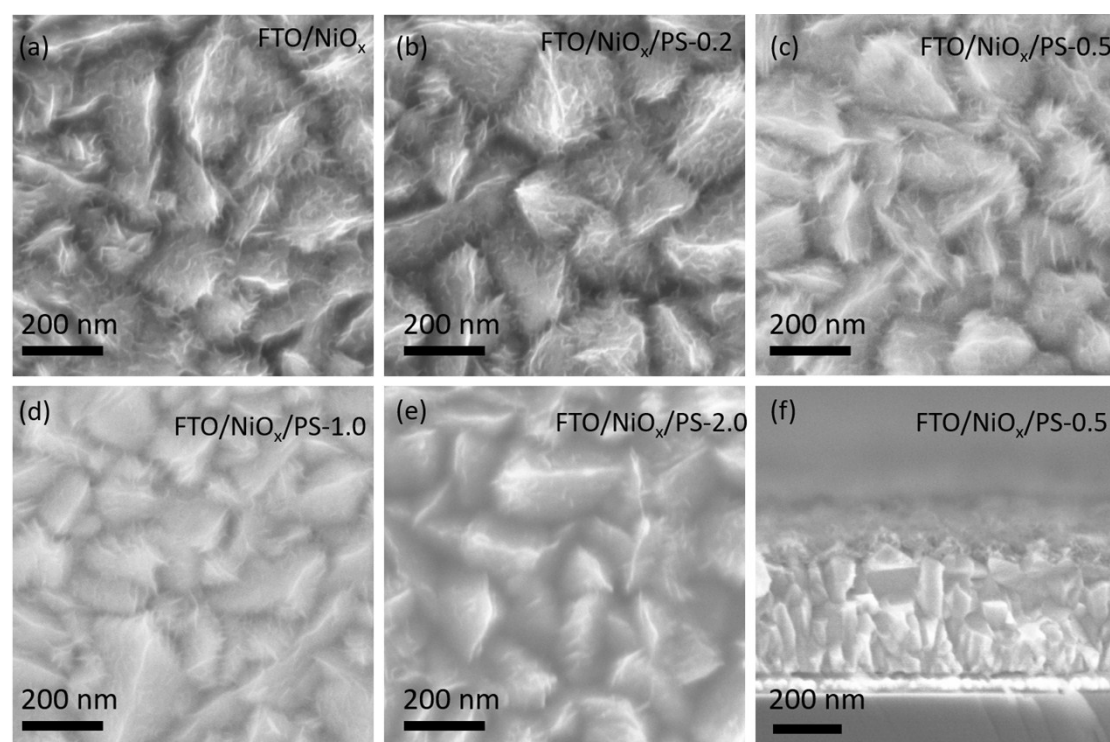


## Supporting Information

# Highly efficient and stable perovskite solar cells via bilateral passivation layers

*Tun Wang, Zhendong Cheng, Yulin Zhou, Hong Liu\*, Wenzhong Shen\**

Key Laboratory of Artificial Structures and Quantum Control (Ministry of Education),  
Institute of Solar Energy, School of Physics and Astronomy, Shanghai Jiao Tong  
University, Shanghai 200240, P. R. China



**Figure S1.** Top-view SEM images of FTO/NiO<sub>x</sub> sample deposited with different PS concentrations (mg mL<sup>-1</sup>) at (a) 0, (b) 0.2, (c) 0.5, (d) 1.0 and (e) 2.0. (f) The cross-sectional SEM image of the FTO/NiO<sub>x</sub> sample deposited with PS at the concentration of 0.5 mg mL<sup>-1</sup>. The numbers in the images represent the PS concentration (mg mL<sup>-1</sup>) dissolved in chlorobenzene.

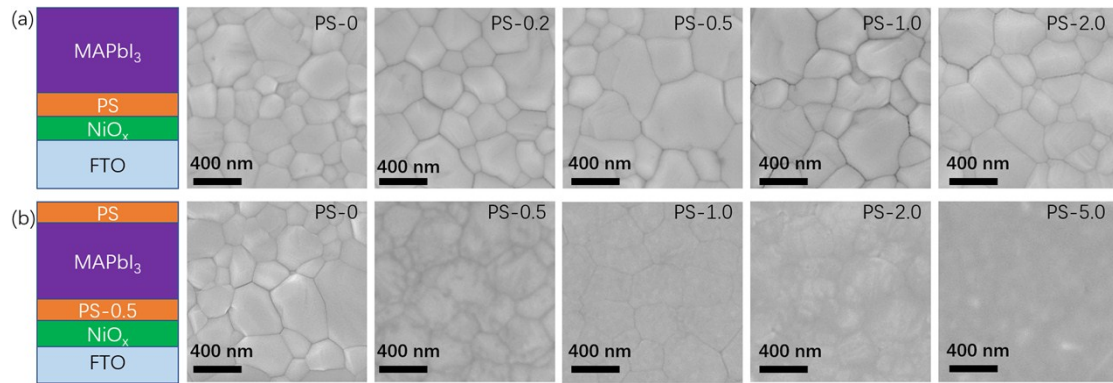


**Figure S2.** Structure diagrams of three different structures, (a) FTO/NiO<sub>x</sub>/PS/MAPbI<sub>3</sub> and (b) FTO/NiO<sub>x</sub>/PS-0.5/MAPbI<sub>3</sub>/PS and the corresponding top-view SEM images. (a) Perovskite films depositing on the bottom passivation layer with different PS concentrations from 0 to 2.0 mg mL<sup>-1</sup>. (b) Perovskite films depositing on the bottom passivation film (PS-0.5) with different PS concentration from 0 to 5.0 mg mL<sup>-1</sup>, here the PS/CB solution acts as the antisolvent.

**Table S1.** Photovoltaic parameters of the PSCs based on bottom passivation layer at various concentrations of PS solution.

$C_{PS}$ (mg mL <sup>-1</sup> )	$V_{OC}$ (V)	$J_{SC}$ (mA cm <sup>-2</sup> )	FF (%)	PCE (%)
0	1.050	21.11	71.74	15.90
0.2	1.099	21.12	72.85	16.91
0.5	1.108	22.45	73.94	18.39
1.0	1.092	22.10	74.36	17.95
2.0	1.062	21.22	64.31	14.49

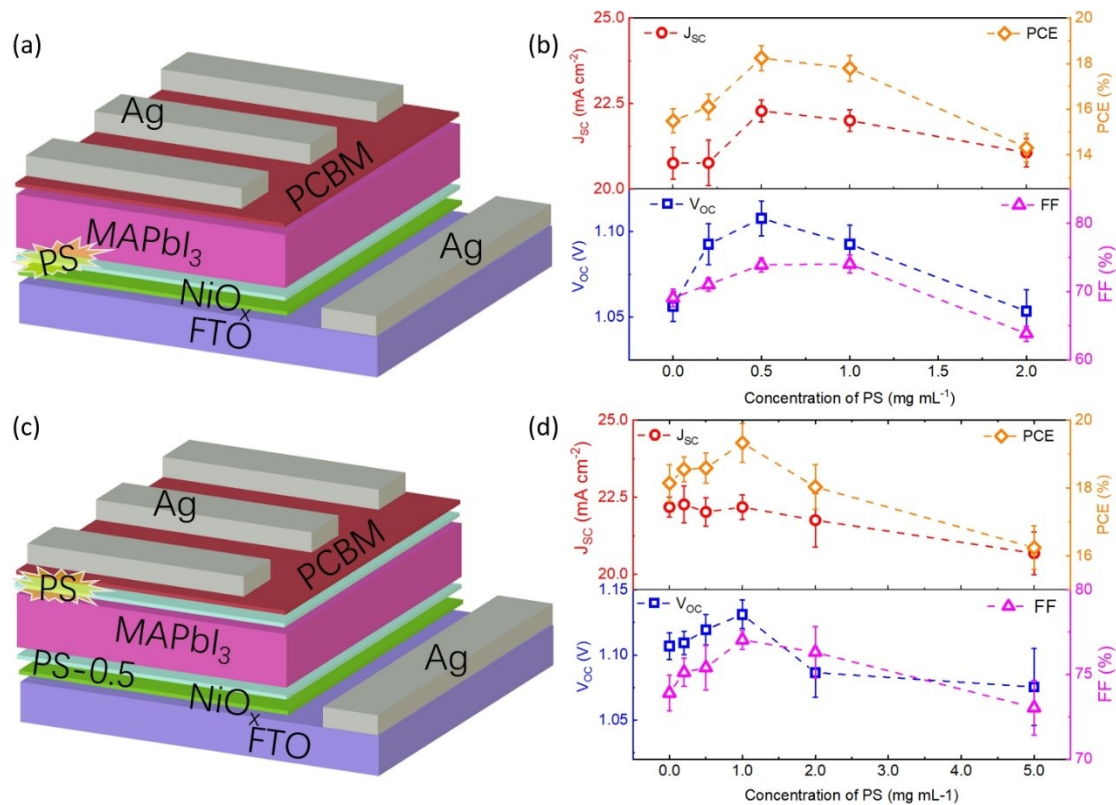


**Figure S3.** Three-dimensional schematic diagram of the PSC with (a) a bottom passivation layer and (c) bilateral passivation layers. Statistics of  $V_{OC}$ ,  $J_{SC}$ , FF and PCE for (b) bottom and (d) bilaterally passivated PSCs with different PS concentrations.

**Table S2.** Photovoltaic parameters of the bilaterally passivated PSCs based on bottom passivation of PS-0.5 and various concentrations for preparing top passivation layer.

$C_{PS}$ (mg mL <sup>-1</sup> )	$V_{OC}$ (V)	$J_{SC}$ (mA cm <sup>-2</sup> )	FF (%)	PCE (%)
0	1.108	22.45	73.94	18.39
0.5	1.129	22.51	75.44	19.17
1.0	1.149	22.51	77.33	19.99
2.0	1.104	21.62	78.22	18.67
5.0	1.094	21.09	74.41	17.16

Table S3. Summarization of the open-circuit voltage for various perovskite solar cells.

Device structure	PCE (%)	$V_{OC}$ (V)	Year/Ref.
ITO/NiO <sub>x</sub> /MAPbI <sub>3</sub> /C <sub>60</sub> /BCP/Ag	18.18	1.09	2018 <sup>1</sup>
ITO/NiO <sub>x</sub> :rGO/MAPbI <sub>3</sub> /PCBM/BCP/Ag	18.90	1.07	2019 <sup>2</sup>
FTO/PEDOT:PSS/MAPbI <sub>3</sub> /HBM/Ag	20.60	1.12	2019 <sup>3</sup>
FTO/TiO <sub>2</sub> /MAPbI <sub>3</sub> /Spiro-OMeTAD/Au	18.70	1.10	2019 <sup>4</sup>
ITO/P3CT-N/MAPbI <sub>3</sub> /IT-4X/s-Bphen/Ag	17.65	1.08	2019 <sup>5</sup>
FTO/Zn:NiO <sub>x</sub> /MAPbI <sub>3</sub> /PCBM/BCP/Ag	18.98	1.08	2019 <sup>6</sup>
ITO/PTAA/MAPbI <sub>3</sub> /C <sub>60</sub> /BCP/Ag	19.50	1.09	2019 <sup>7</sup>
ITO/SnO <sub>2</sub> /MAPbI <sub>3</sub> /Spiro-OMeTAD/P3HT/Au	18.50	1.10	2019 <sup>8</sup>
FTO/TiO <sub>2</sub> NW/MAPbI <sub>3</sub> /Spiro-OMeTAD/Au	19.50	1.12	2019 <sup>9</sup>
FTO/TiO <sub>2</sub> MCP/MAPbI <sub>3</sub> /Spiro-OMeTAD/Au	20.08	1.09	2019 <sup>10</sup>
FTO/TiO <sub>2</sub> /MAPbI <sub>3</sub> /Spiro-OMeTAD/Au	18.59	1.11	2019 <sup>11</sup>
FTO/NiO <sub>x</sub> /PS/MAPbI <sub>3</sub> /PS/PCBM/Ag	19.99	1.149	Our work

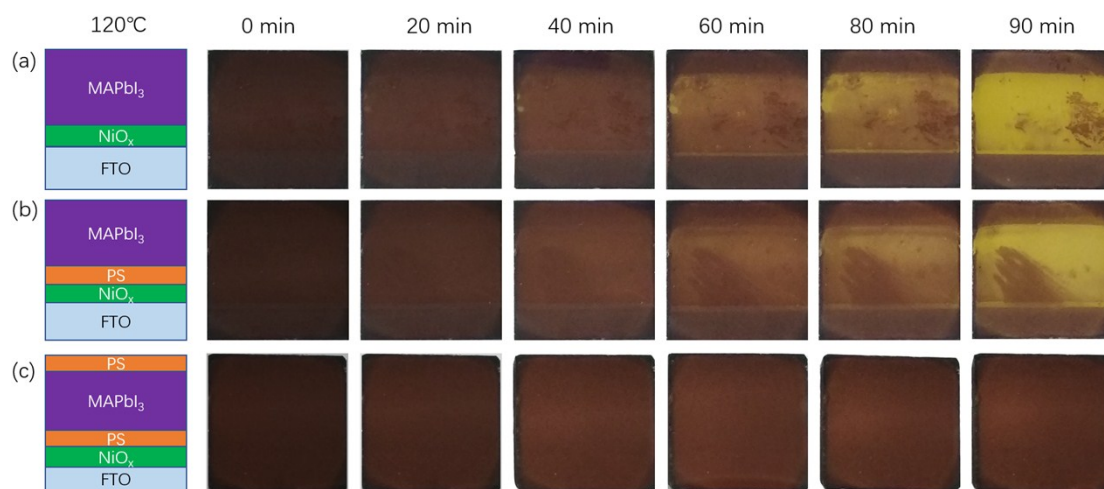


Figure S4. Photographs of (a) the pristine perovskite film without passivation layers

and (b) bottom and (c) bilateral-passivated perovskite films annealed at 120 °C in ambient air (humidity 60%) for different times.

## References

- 1 W. Chen, Y. Wu, J. Fan, A. B. Djurišić, F. Liu, H. W. Tam, A. Ng, C. Surya, W. K. Chan, D. Wang and Z.-B. He, *Adv. Energy Mater.*, 2018, **8**, 1703519.
- 2 M. Li, X. Xu, Y. Xie, H.-W. Li, Y. Ma, Y. Cheng and S.-W. Tsang, *J. Mater. Chem. A*, 2019, **7**, 9578-9586.
- 3 D. Yang, X. Zhang, K. Wang, C. Wu, R. Yang, Y. Hou, Y. Jiang, S. Liu and S. Priya, *Nano Lett.*, 2019, **19**, 3313-3320.
- 4 C. Wu, K. Wang, X. Feng, Y. Jiang, D. Yang, Y. Hou, Y. Yan, M. Sanghadasa and S. Priya, *Nano Lett.*, 2019, **19**, 1251-1259.
- 5 X. Liu, X. Li, Y. Zou, H. Liu, L. Wang, J. Fang and C. Yang, *J. Mater. Chem. A*, 2019, **7**, 3336-3343.
- 6 J. Liu, N. Li, J. Jia, J. Dong, Z. Qiu, S. Iqbal and B. Cao, *Sol. Energy*, 2019, **181**, 285-292.
- 7 B. Li, Z. Chen, H. Yao, X. Guan, Z. Yu, F. Halis Isikgor, H. Coskun, Q. H. Xu and J. Ouyang, *Nanoscale*, 2019, **11**, 3216-3221.
- 8 G. Jang, H. C. Kwon, S. Ma, S. C. Yun, H. Yang and J. Moon, *Adv. Energy Mater.*, 2019, DOI: 10.1002/aenm.201901719, 1901719.
- 9 W. Q. Wu, J. F. Liao, Y. Jiang, L. Wang and D. B. Kuang, *Small*, 2019, **15**, 1900606.
- 10 Y. Wang, M. Li, H. Li, Y. Lan, X. Zhou, C. Li, X. Hu and Y. Song, *Adv. Energy Mater.*, 2019, DOI: 10.1002/aenm.201900838, 1900838.
- 11 J. W. Lee, H. Yu, K. Lee, S. Bae, J. Kim, G. R. Han, D. Hwang, S. K. Kim and J. Jang, *J. Am. Chem. Soc.*, 2019, **141**, 5808-5814.